Journal of Applied Polymer Science

Amphoteric Hydrolyzed Poly(acrylamide/dimethyl diallyl ammonium chloride) as a Filtration Reducer Under High Temperatures and High Salinities

Ling Lin, Pingya Luo
State Key Laboratory of Oil and Gas Reservoir Geology and Exploitation, College of Chemistry and Chemical Engineering, Southwest Petroleum University, Chengdu 610500, Sichuan, People's Republic of China
Correspondence to: L. Lin (E-mail: cowbolinling@aliyun.com)

ABSTRACT: Poly(acrylamide/dimethyl diallyl ammonium chloride) (PAD) samples were synthesized via solution polymerization. Hydrolyzed poly(acrylamide/dimethyl diallyl ammonium chloride) (HPAD) was prepared with NaOH as a hydrolyzation agent. Both PAD and HPAD were characterized by IR and NMR spectroscopy. Na_2SO_3 was added to slow down the decomposition of HPAD under elevated temperatures. The rheological and filtrate properties of the drilling fluids were investigated in saltwater mud. We found that 30 wt % NaCl hampered those properties. Increasing HPAD's percentage in the clay suspensions reduced the filtrate volumes and whereas increased the viscosities. A greater amount of HPAD added to the saltwater mud resulted in a smaller particle medium size and caused the ζ potential to move toward a less negative value. The hydrolysis degree of HPAD needed to be controlled in a proper range to optimize the reduction in filtration. Scanning electron microscopy photos showed that HPAD was distributed in the surface of the high-temperature and high-pressure filter cake as bridges. The drilling fluids with 3.5 wt % HPAD had an excellent tolerance to 30 wt % NaCl and a temperature of 200°C. © 2014 Wiley Periodicals, Inc. J. Appl. Polym. Sci. **2015**, *132*, 41581.

KEYWORDS: applications; clay; oil and gas; polyelectrolytes; thermal properties

Received 16 April 2014; accepted 30 September 2014
DOI: 10.1002/app.41581

INTRODUCTION

Fluid loss reducers act as important components of drilling fluids in the oil and gas industry.[1,2] One of the main functions of filtration reducers is to help in the formation of a thin and dense cake on the wall of the borehole; this inhibits water from leaking into the formation and maintains the wellbore stability.[3,4] Reservoirs of high temperature and high salinity put forward a challenge for oilfield working fluids, including filtration reducers.[5,6] Oil-based mud is one of the best choices in such harsh conditions because of its resistance to temperatures as high as 260°C and its low filtration. Environmental legislation, however, has imposed increasing restrictions on the application of oil-based fluids.[7]

Traditional fluid loss reducers for water-based drilling fluids are based on modified natural products, such as cellulose, starch, humic acid, and lignite.[8–13] The use of filtrate additives, however, has been confined because of either their vulnerability to salt or a need for chromium ions to form metallic complexes, which have caused great damage to the environment.

Polymers, particularly polyelectrolyte carrying charges,[14] have been drawing growing attention as oilfield working fluid additives in recent studies to deal with high-temperature and high-salinity challenges to water-based muds. The main trend of filtrate additives' design is to turn them to polyelectrolytes with only anionic groups. This type of polyelectrolyte attaches to bentonite's surface via hydrogen bonds or van der Waal's forces and protects clay from aggregation by its anionic groups; this shows that the interaction between polyelectrolyte and clay flakes was unstable under high temperature (e.g., 200°C). Various polyelectrolytes with sulfonic groups have been synthesized to tackle with the high temperature and low salinity problem; these include sulfomethylated phenolic resin;[1] the terpolymer of disodium itaconate, acrylamide (AM), and sodium 2-acrylamido-2methyl-1-propane sulfonate;[15] the forpolymer of *N*-vinyl pyrrolidone (NVP), disodium itaconate, AM, and 2-acrylamido-2-methyl-1-propane;[16] and polycomplexes of the terpolymer of AM, acrylic acid, and 2-acrylamido-2-methyl propane sulfonic acid (AMPS) with aluminum citrate.[17] Other polymers have been produced to face the challenge of high-temperature and saturated salinity conditions, including starch-*graft*-polyacrylamide (PAM)[18] and the forpolymer of AM, AMPS, NVP and organosilicon monomer.[19] Polymers with only polar groups rather than charged groups [e.g., poly(methyl methacrylate-*co*-vinyl acetate)] have also been synthesized to

study their potential to be filtration controllers in freshwater muds.[20] Lightly branch poly(vinyl alcohol) was produced in laboratory by Han and Zhang[21] to function as a fluid loss additive in a salt-free cement slurry.

In previous studies on fluid loss reducers, not only rheological properties but also American Petroleum Institute (API) filtration and high-temperature and high-pressure (HTHP) filtration were the main methods used to evaluate the effectiveness of synthetic fluid loss reducers. Among recent reports on filtration additives designed for the formation conditions of high temperature ($\geq$200°C) and nearly saturated brine, Chu et al.[19] synthesized the forpolymer of AM, AMPS, NVP, and organosilicon monomer, which proved quite effective in the API filtration test. They prepared brine-saturated mud with 8.0 wt % bentonite and 1.0 wt % forpolymer. The API filtration of this mud after hot rolling under 220°C for 16 h was nearly 37.5 mL, whereas the apparent viscosity (η_a) and plastic viscosity (η_p) were 14.0 and 10.0 mPa s, respectively; API filtration of this mud after aging under 200°C for 16 h was nearly 14.0 mL, whereas η_a and η_p were 39.0 and 27.0 mPa s, respectively.

Polyampholyte,[22] with anionic groups and cationic groups in the same polymer chain, also shared the ability to control the filtration of water-based drilling fluids. High salinity screened the intramolecular and intermolecular coulomb forces so that part of cationic groups in polyampholyte could be absorbed to the negatively charged bentonite surface. The electrostatic forces were stronger than hydrogen bonds or van der Waals' forces, which indicated that polyampholyte had a more stable interaction with clay plates under high temperatures.

In this study, we examined the potential of polyampholyte as a fluid loss reducer for water-based drilling fluids with hydrolyzed poly(acrylamide/dimethyl diallyl ammonium chloride) (HPAD) as a filtrate additive, trying to draw more attention from peers to polyampholyte's application in drilling fluids. The influence of the hydrolysis degree on the filtration performance was also studied. Another aim of this study was to reduce API filtration to less than 5 mL and the HTHP (carried out under 180°C) filtration to less than 20 mL after an aging treatment with HPAD as a fluid loss reducer of saltwater mud. No research has been reported on the use of HPAD as a fluid loss controller. The copolymer of AM and dimethyl diallyl ammonium chloride (DMDAAC), as well as the terpolymer of AM, acrylic acid, and DMDAAC, are used as a superabsorbent,[23] in hair care products,[24] a retention aid in papermaking,[25] for clay swelling inhibition,[26] and as a polymer flooding agent.[27]

In this study, IR, NMR, and titration were used to determine the chemical composition and quantify each functional group's content in the polymers. Thermogravimetric analysis (TGA) and intrinsic viscosity measurement were used to test the polymers' heat-resistant abilities. The particle size distribution was introduced to evaluate the clay suspension's ability to form a dense filtrate cake and for filtration reduction on the basis of one rule that the median size of the bridging particle should be equal to or slightly greater than one-third of the median pore size of the formation simulated by filter paper in the HTHP experiment;[28,29] A ζ potential test was performed to reveal the interactions between the polymer and clay flakes. If the ζ potential of the clay plates shifted toward a more negative value, the probability of bentonite's aggregation was reduced, and the rheological properties of the clay suspension could be controlled better. API and the HTHP filtrate experiments were carried out to quantify the filtration of the saltwater mud with and without additives.

EXPERIMENTAL

Materials

AM [analytical reagent (AR)], $NaHSO_3$ (AR), APS (AR), methyl orange (AR), indigo carmine (AR), $AgNO_3$ (AR), K_2CrO_4 (AR), NaOH (AR), Na_2SO_3 (AR), Na_2CO_3 (AR), NaCl (AR), and ethanol (AR) were purchased from Chengdu Kelong Chemical Co. (China) and were used as received. DMDAAC (60 wt % in water, AR) was provided by Sinopharm Chemical Reagent Co. (China) and were used as received. The bentonite used for preparing drilling fluids in this study was provided by Zhongfei Xiazijie Bentonite Co. (Xinjiang, China) and was used as received.

Synthesis and Characterization of the Polymers

AM and DMDAAC with a weight ratio of 2:1 and a magnetic rotor were added to a four-necked round-bottom flask equipped with a thermometer and a nitrogen inlet tube. APS and $NaHSO_3$ solutions of given concentrations, namely, a 1:1 molar ratio, were prepared separately. After degassing oxygen with nitrogen for 20 min and controlling the initiation at 50°C in a deionized water bath with a magnetic stirrer, we initiated the polymerization by injecting the initiator solutions into the reaction mixture under stirring. The concentration of the monomers was 30 wt % on the basis of the total weight of the reaction system. The concentration of initiators was 0.1 wt % on the basis of the total weight of the monomers. We let the reaction proceed for 10 h to get a high conversion of monomers. The poly(acrylamide/dimethyl diallyl ammonium chloride) (PAD) products were purified by precipitation in ethanol several times. The samples synthesized via the previous procedure were dried for 24 h at 60°C *in vacuo* (10^{-3} Torr) and were then used for the tests mentioned in this article.

The PAD synthesized via the previous method; sodium hydroxide with 5.5:1, 4:1, 3:1, and 2:1 weight ratios; and deionized water were added to a one-necked, round-bottom flask equipped with a reflux condensation tube. Then, hydrolysates with various hydrolysis degrees were obtained, namely, HPAD-1, HPAD-2, HPAD-3, and HPAD-4. The concentration of PAD was 5 wt % on the basis of the total weight of the reaction system. The reaction temperature and duration were 85°C and 24 h, respectively. HPAD was purified via the same procedure used for PAD.

PAM and poly(dimethyl diallyl ammonium chloride) (PDM) were prepared and purified with the same methods used for PAD.

The intrinsic viscosities of PAD and HPAD were determined in a 1 mol/L NaCl aqueous solution with an Ubbelohde capillary viscometer (Shanghai Shenyi Glass Instrument Co., Ltd., China) at 30 $\pm$ 0.1°C. The cationicity of HPAD was determined by the titration of a PAD aqueous solution with an $AgNO_3$ aqueous

solution (0.05 mol/L) with K_2CrO_4 (5 wt % in water) as an indicator. When the color of solution changed from bright yellow to brick red, the titration end point was reached. The anionicities of PAD and HPAD were characterized by titration with HCl (0.1 mol/L) with methyl orange (0.1 wt % in water) and indigo carmine (0.25 wt % in water) as indicators. The end point was determined by the change in the HPAD solution's color from yellowish green to French gray.

The IR spectra of the polymers were obtained with a WQF-520 Fourier transform infrared spectrometer (Beijing Rayleigh Analytical Instrument Corp., China).

The ^{1}H-NMR spectra of the polymers in D_2O were obtained with a Bruker Ascend 400-MHz NMR spectrometer.

The samples' thermal properties were tested with a Mettler-Toledo TGA/SDTA851^e instrument. The testing temperature range was from 40 to 600°C, the heating rate was 10°C/min, and the experimental atmosphere included both air (simulated by a mixture of N_2 and O_2 with a 4:1 volume ratio in this study) and N_2. To figure out what had happened to the functional groups of HPAD under different temperatures, we also used a TGA device in which HPAD-2 experienced temperature ranges of 40–250, 40–350, and 40–500°C at a heating rate of 10°C/min at both N_2 and air atmospheres, and we then obtained the IR spectra of the samples with the various heat treatments.

Preparation and Aging of the Mud

The procedure of mud preparation and the aging treatment was designed on the basis of previous work.[7,15,16,18,19]

The freshwater-based mud, containing 5 wt % bentonite, 0.25 wt % Na_2CO_3, and tap water, was prepared by stirring at a certain ratio and aging for 24 h at room temperature. The saltwater-based mud was prepared by a similar procedure followed by the addition of various quantities of HPAD, 30 wt % NaCl, and 1 wt % Na_2SO_3 with stirring at 1500 rpm and aging for another 24 h at room temperature.

The aging experiments of the mud sealed in pressure vessels were carried out in a BRGL-7 type rolling oven through hot rolling at 200°C for 16 h. This step was introduced to simulate the drilling fluids' duration at high temperatures underground. The next step in the procedure was to cool the mud to room temperature and stir it for 15 min at 10,000 rpm to simulate the mud's flow through the bit. After that, the mud went on being rolled for another 16 h at 60°C; the mud's circulation in the annulus between the drill pipe and the wall of the hole or casing was similar.

Mud Property Tests

Mud property tests were carried out in accordance with API specifications. The API filtrate volume of mud was measured with an SD3 medium-pressure filtration apparatus made by Qingdao Tongchun Co. (China). The HTHP filtrate volume of the mud was measured at 180°C, as per API specifications, with an apparatus provided by Shenyang Jinouke Co. (China). The pore size of the filter paper used in the HTHP filtration experiment to simulate the formation was less than 20 μm in accordance with SY/T 5677-1993, one of China's industrial standards.

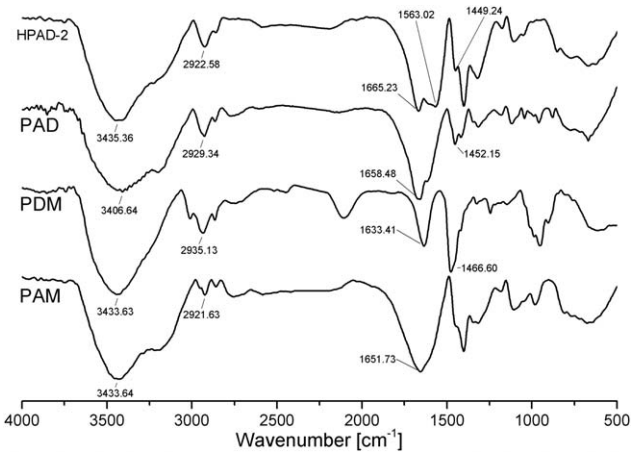

Figure 1. IR spectra of PAM, PDM, PAD, and HPAD-2.

All of the mud needed to be stirred at 1500 rpm before viscosity measurement, in which the testing temperature was 30 ± 0.5°C. The rheological properties of the mud, namely, η_a, η_p, and yield point (τ_0), were determined and calculated by the measurement of the viscosity at two rotating rates, 300 and 600 rpm, by a ZNN-D6 type rotating viscometer, according to a related previous work.[7]

Particle Size Measurement

Both the size distribution and medium size of the clay particles were obtained with a Malvern Mastersizer 2000. All of the samples were dispersed by ultrasonic agitation before size measurements with the maximum concentration set at 0.1 g/L.

ζ Potential Measurement

The ζ potential of all of the mud in this article was determined with a Brookhaven ZetaPALS 190 Plus instrument. The dispersions were prepared by the dilution of loss volume test samples to 0.1 wt % solid.

Microstructure Observation

The microstructure of the filter cakes in the API and HTHP filter volume experiments was observed with a FEI QUANTA450 scanning electron microscope.

RESULTS AND DISCUSSION

Structure Characterization of the Polymers

Figure 1 shows the IR spectra of PAM, PDM, PAD, and HPAD-2.

The —NH_2 stretching vibration absorption peak appeared around 3430 cm^{-1}; this was the characteristic absorption of the AM segments. The band near 2930 cm^{-1} was the characteristic peak of the C—H of methylene and methylidyne in the AM and DMDAAC units. The absorption at about 1650 cm^{-1} corresponded to the —$CONH_2$ in PAM, PAD, and HPAD-2. The band around 1560 cm^{-1} in the HPAD-2 spectrum was the characteristic peak of COO^-; this demonstrated that part of —$CONH_2$ was successfully hydrated to —COO^- in HPAD-2. The peak near 1460 cm^{-1} was related to dual methyl bonding

Table I. Characterized Peaks and Corresponding Chemical Groups

Functional group	$-NH_2$	C—H	$-CONH_2$	$-COO^-$	$-CH_3-N^+$
Frequency (cm^{-1})	3430	2930	1650	1560	1460

with $-N^+$ and manifested the existence of the DMDAAC segments in PAD and HPAD-2.

Table I includes several characterized peaks of functional groups as discussed later.

The ^{1}H-NMR spectra of PAM, PDM, PAD, and HPAD-2 are presented in Figure 2. According to previous work on PAD,[30,31] peaks in the spectrum were identified, as discussed later.

The peaks at 1.53 and 1.64 ppm corresponded to the $-CH_2$ of the AM segments, whereas the ones at 2.08 and 2.22 ppm were the characteristic peaks of the proton in the —CH of the AM units. The signals between 2.60 and 3.20 ppm were assigned the hydrogen of methylene groups linked with $-N^+$; this provided evidence of the DMDAAC units' existence. The resonance around 3.75 ppm was caused by $-CH_2$ attached to $-N^+$. All of those peaks in PAM and poly dimethyl diallyl ammonium chloride (PDMDAAC) existed in the PAD and HPAD-2 ^{1}H spectra. This demonstrated that the AM monomers and DMDAAC monomers copolymerized successfully. The residual ethanol's absorption peaks appeared at 1.10 and 3.55 ppm.

The compositions of PAD and HPAD are given in Table II. Because the existence of COO^- may have affected the titration results of HPAD's cationicity, HPAD was supposed to have the same content of cationic groups as PAD. PAD had a net positive charge, whereas HPAD had a net negative charge. The intrinsic viscosity of HPAD was higher than that of PAD as a result of the hydrolyzation of PAD introducing COO^- into the polymer chains. The intrinsic viscosity of hydrolysate decreased as the hydrolysis degree increased. The reason was that when more COO^- was introduced into the polymer chain, the higher possibility that coulomb interactions between the DMDAAC units and COO^- units could occur intramolecularly and intermolecularly; this hampered the stretching of polymer chains and led to a reduction in the intrinsic viscosity.

Table II. Structural Properties of PAD and HPAD

Polymer	Intrinsic viscosity (dL/g)	Cationicity (mol %)	Anionicity (mol %)
PAD	3.45	10.3	0
HPAD-1	4.42	10.3	30.0
HPAD-2	4.06	10.3	40.4
HPAD-3	3.73	10.3	49.6
HPAD-4	3.48	10.3	51.8

Thermal Analysis of HPAD-2

The TGA curves, together with the dynamic thermal analysis curves, of HPAD-2 under N_2 and air are presented in Figure 3.

According to the TGA curves of HPAD-2 in N_2 and air atmospheres, HPAD-2 had a lower thermal stability in air as a result of O_2's participation in speeding up the decomposition of HPAD-2. The polymer exhibited four stages of decomposition under N_2. The first one began at room temperature and ended around 230°C. Ten percent of its weight was lost as a result of the volatilization of water, ethanol, and the residual monomers. The second stage occurred in the range 230–350°C, during which the sample suffered another loss of 10 wt %. Not only the amide and carboxyl groups in AM segments but the five-membered rings of DMDAAC units were decomposed in this phase. The decomposition of the HPAD-2 backbone along with the progressively carbonization dominated the third phase, during which 30% of the total weight turned into a variety of gases. The little fluctuation in this stage was caused by the volume expansion of the samples. In the last stage, a small change in the sample weight was observed from 480 to 600°C; it corresponded to further carbonization.

The presence of O_2 accelerated HPAD-2's weight loss at high temperatures. The sample weight dropped to around 90% of its original value when the temperature only went up to 100°C; this revealed that the amide and carboxyl groups and five-membered rings were more unstable under air than under N_2.

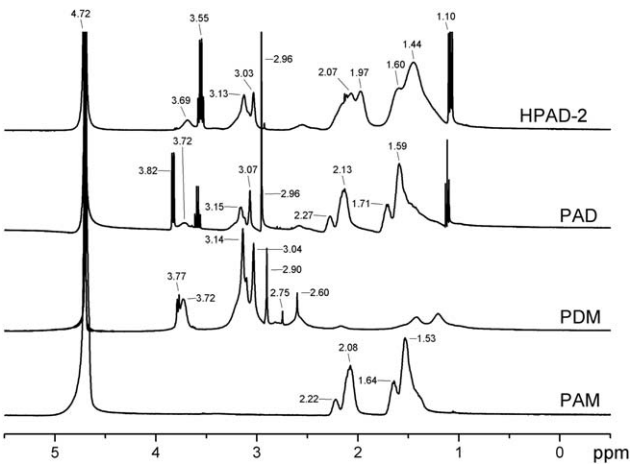

Figure 2. NMR spectra of PAM, PDM, PAD, and HPAD-2.

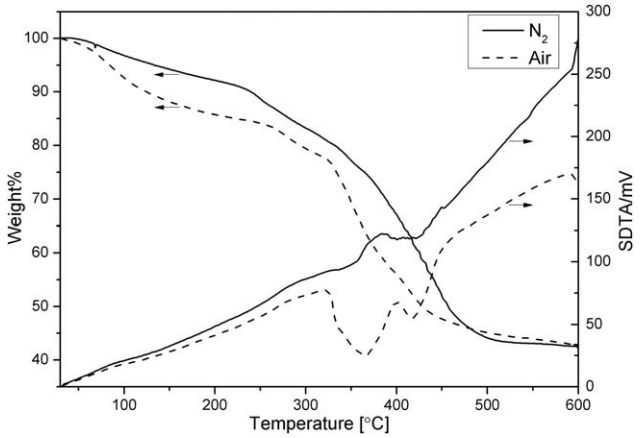

Figure 3. TGA and dynamic thermal analysis curves of HPAD-2 under N_2 and air.

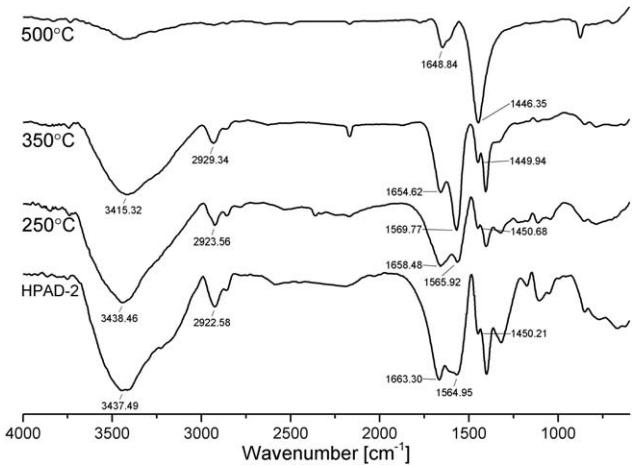

Figure 4. IR spectra of the HPAD-2 samples heated to various temperatures under N_2.

A moderate change in the weight percentage occurred in the range 100–280°C. HPAD-2 continued to be less stable under air until the temperature reached 470°C. Carbonization was observed between 470 and 600°C; this was similar to that of HPAD-2 under N_2.

Figure 4 shows the IR spectra of HPAD-2 with heating to 250, 350, and 500°C under N_2 and those of the untreated samples.

The initial color of the HPAD-2 sample was light yellow when no treatment was carried out. The appearance of the sample remained unchanged even after it was heated to 250°C, whereas all of the characteristic peaks of the preheated HPAD-2 still remained. As the temperature was increased further, the samples experienced an expansion in volume. The color of HPAD-2 turned yellow after it was heated to 350°C. The proportion of $-NH_2$, with corresponding peaks at roughly 3430 cm^{-1}, decreased markedly; this revealed that the amide groups suffered a higher decomposition rate than the carboxyl groups in the range 250–350°C. It was obvious that the peaks of the $-NH_2$ and carboxyl groups almost vanished from the IR spectrum after heating to 500°C. The polymers underwent a process of carbonization, with a further expansion in volume in the company of color darkening. Only part of methyl groups bonding with $-N^+$, characterized by the peak around 1460 cm^{-1}, and a small amount of amide groups, with characteristic peaks at 1648 cm^{-1}, were observed in the black ash after heating to 500°C under N_2.

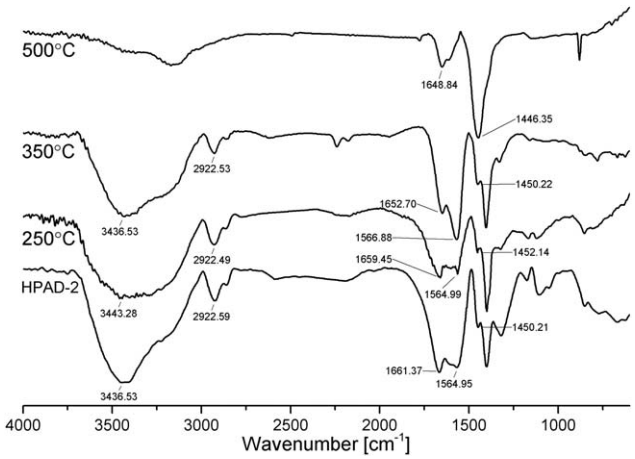

Figure 5. IR spectra of the HPAD-2 samples heated to several temperatures under air.

Table III. Influence of Na_2SO_3 on the Intrinsic Viscosity of the HPAD-2 Aqueous Solution After the Aging Treatment

HPAD-2 (wt %)	Na_2SO_3 (wt %)	Intrinsic viscosity (dL/g)
3.5	0	52.96
3.5	0.5	101.95
3.5	1	167.19

Figure 5 shows the IR spectra of HPAD-2 with heating to 250, 350, and 500°C under air and those of the original samples.

The existence of O_2 darkened the color of HPAD-2 after different treatments. HPAD-2 appeared to be yellow after it was heated to 250°C, with all of the characteristic peaks of the unheated HPAD-2 still remaining. The color of samples turned into yellowish white after the samples were heated to 350°C, but no expansion in the volume could be found. The sample changed to black ash as the temperature was increased to 500°C. Methyl groups bonding with $-N^+$ related to the peak at 1460 cm^{-1} and amide groups with a peak at 1648 cm^{-1} were observed in the black ash under air; this revealed that methyl group bonding with $-N^+$ was more stable than carboxyl groups carrying a negative charge under high temperature in both the N_2 and air atmospheres.

The weight losses of HPAD-2 under N_2 and air were 7 and 15%, respectively, after they were heated to 200°C on the basis of the TGA results. The main characteristic peaks in the original spectrum of the unheated products were still be found in the IR spectra of the samples heated to 250°C under both N_2 and air atmospheres. The reason for the mass loss distinction was that the amide and carboxyl groups decomposed at a higher rate with O_2's presence. In water, the process of degradation might have sped up because of the existence of dissolved oxygen. If amide and carboxyl groups decompose during aging, the viscosity of the solution drops spectacularly. One anti-oxygen agent, therefore, was needed to inhibit HPAD-2 from degrading too fast in mud. Na_2SO_3 is an efficient antioxidant for eliminating free oxygen in solution;[32] with its addition, the degradation of HPAD-2 was slowed down.

Table IIIshows the experiment carried out to determine the influence of Na_2SO_3's existence on the intrinsic viscosity of the HPAD-2 aqueous solution (3.5 wt %) after aging at 200°C for 16 h. The data in Table III reveal that the value of the intrinsic viscosity of the HPAD-2 solution with Na_2SO_3 was higher than that without Na_2SO_3. As the percentage of Na_2SO_3 rose, the intrinsic viscosity retained after the rolling treatment under 200°C increased; this demonstrated that Na_2SO_3 functioned effectively in reducing the harm to the polymer chain in water by O_2.

As per Table IV, Na_2SO_3 also did well in maintaining η_a, η_p, and τ_0 against the aging process. τ_0 of HPAD-2 mud with 1 wt %

Table IV. Influence of Na_2SO_3 on the Rheological Behaviors of the Saltwater HPAD-2 Mud

		η_a (mPa s)			η_p (mPa s)			τ_0 (Pa)			API loss (mL)	HTHP loss (mL)
HPAD-2 (wt %)	Na_2SO_3 (wt %)	◇	△	▽	◇	△	▽	◇	△	▽	▽	▽
3.5	0	—	30.5	25.0	—	28.0	25.0	—	2.56	0	21	189.3
3.5	1.0	—	—	81.0	—	—	59.0	—	—	22.48	2.2	17.4

◇, measurements were taken before aging; △, measurements were taken after aging at 200°C for 16 h; ▽, measurements were taken after aging at 60°C for 16 h; —, the sample exceeded the measuring range of the rotating viscometer.

Na_2SO_3 was nearly 10 times of that without antioxidant. The increment of η_a and η_p resulted in better API and HTHP filter volumes; their values were one tenth of the figures with no anti-oxygen agent.

Influence of NaCl's Addition

The existence of salts, such as NaCl, considerably affected the mud's rheological properties. η_a, η_p, and τ_0 slumped to less than half of their original values after aging even with only 4 wt % NaCl, according to the research done by Wu et al.[15] Salts' harm to the mud's properties was also investigated by Zhang and Yan.[33] Their experimental result was that even 0.7–1.2 wt % NaCl inflicted significant damage to η_a, η_p, and τ_0, especially after aging.

As the concentration of NaCl increased, the rheological properties of the base mud dropped progressively according to Table V. The higher the proportion of sodium chloride was in the mud, the smaller the thickness of the particles' electric double layer became. The clay flakes in the saltwater mud aggregated to some extent because of the high concentration of NaCl. Both the API and HTHP filtration of the base mud, consequently, performed badly because of the considerable excess of salt. A concentration of 30 wt % NaCl and Cl^- dissociated from the DMDAAC segments and Na^+ from the hydrolyzed AM segments made an atmosphere of nearly saturated electrolyte in this study's saltwater mud. η_a, η_p, and τ_0 all dropped markedly, whereas APD and HTHP performed badly when the content of NaCl reached 30 wt %.

Effects of the HPAD-2 Concentration on the Saltwater Mud's Properties

The effects of the HPAD-2 concentration on the rheological behaviors and filtration of saltwater mud are listed in Table VI.

In the absence of HPAD, saltwater mud had low η_a, η_p, and τ_0 values but high filtration. Only a small addition of HPAD-2 (0.5% in weight proportion) improved the mud's API filtration performance. The rise of the polymer concentration significantly decreased the API filtration, although it increased η_a, η_p, and τ_0 of the drilling fluids. A low proportion of HPAD-2 in mud indicated excessive losses of fluid. The HTHP filtration stayed high even when the additive's weight percentage increased from 0 to 2%. When its percentage reached 3.5%, the API filtration slumped to 2.2 mL, whereas the HTHP filtration was merely 17.4 mL; with this, we achieved the goal we set in this study. When the additive's proportion in the drilling fluid continued to rise, namely, to 4.0 and 5.0 wt %, both the viscosity and τ_0 grew bigger, whereas the API and HTHP filtrate volume continued to drop, but the variation was relatively small. A concentration of 3.5 wt % HPAD-2 was enough to reduce the mud's API filtration to less than 5 mL and the HTHP filtrate volume to less than 20 mL after the heat treatment.

Particle Size Test Results

The particle sizes of the saltwater mud with a series of HPAD-2 weight percentage are listed in Table VII. Of the data later, 10, 50, and 90% of all particles had a diameter less than $d(0.1)$, $d(0.5)$, and $d(0.9)$, respectively.

The distribution of clay flakes in the saltwater mud, characterized by $d(0.1)$, $d(0.5)$, and $d(0.9)$ together, became wider after HPAD-2's addition as bridges formed among bentonite. Rolling at 200°C for 16 h resulted in a decrease in three sizes of the clay flakes because the high temperature destroyed part of the polymer bridges across adjacent particles. The following aging treatment, at 60°C for 16 h, slightly broadened the size distribution with the additive's concentration in the range of 0.5–2 wt % and continued to narrow the particle distribution when its concentration exceeded 2 wt %. On balance, an increase in HPAD-2's percentage in the mud led to shifts in $d(0.1)$, $d(0.5)$,

Table V. Rheological Behavior of the Freshwater and Saltwater Muds Without HPAD

	η_a (mPa s)			η_p (mPa s)			τ_0 (Pa)			API loss (mL)	HTHP loss (mL)
NaCl (wt %)	◇	△	▽	◇	△	▽	◇	△	▽	▽	▽
0	10.5	10.5	8.5	5.0	6.0	6.0	5.62	4.60	2.56	26.5	71.5
5	10.0	6.0	4.5	4.0	4.0	4.0	6.13	2.04	0.51	222.2	All lost
10	9.0	5.0	4.5	4.0	4.0	4.0	5.11	1.02	0.51	All lost	All lost
20	8.0	4.5	4.0	3.0	3.0	4.0	5.11	1.53	0	All lost	All lost
30	7.0	4.0	3.5	5.0	3.0	3.0	2.04	1.02	0.51	All lost	All lost

◇, measurements were taken before aging; △, measurements were taken after aging at 200°C for 16 h; ▽, measurements were taken after aging at 60°C for 16 h; —, the sample exceeded the measuring range of the rotating viscometer.

Table VI. Rheological Behavior of the Saltwater Mud with HPAD-2

	η_a (mPa s)			η_p (mPa s)			τ_0 (Pa)			API loss (mL)	HTHP loss (mL)
HPAD-2 (wt %)	◇	△	▽	◇	△	▽	◇	△	▽	▽	▽
0	7.0	4.0	3.5	5.0	3.0	3.0	2.04	1.02	0.51	All lost	All lost
0.5	27.0	12.5	10.5	24.0	10.0	7.0	3.07	2.56	3.58	59.1	All lost
1.0	56.5	16.5	16.0	39.0	13.0	11.0	17.89	3.58	5.11	42.4	All lost
2.0	—	29.5	27.0	72.0	24.0	22.0	54.17	5.62	5.11	12.9	74.6
3.5	—	—	81.0	—	—	59.0	—	—	22.48	2.2	17.4
4.0	—	—	85.0	—	—	60.0	—	—	25.55	2.4	15.0
5.0	—	—	86.5	—	—	62.0	—	—	25.04	2.0	13.3

◇, measurements were taken before aging; △, measurements were taken after aging at 200°C for 16 h; ▽, measurements were taken after aging at 60°C for 16 h; —, the sample exceeded the measuring range of the rotating viscometer.

and $d(0.9)$ toward smaller value, whereas the particle dispersity became narrower after the aging treatment.

The analysis of the previous results follows. First, 30 wt % NaCl provided a high screening force to break the intramolecular and intermolecular coulomb interactions between the cationic groups and anionic groups. Part of the quaternary ammonium of the DMDAAC segments in polymer chains, carrying positive charges, was absorbed to the negatively charged surface of the particles. The carboxyl groups in the dehydrated AM segments with negative charges repulsed each other and interacted actively with water molecules to widen the electric double layer around the clay particles. Bridging, the main interaction between amphoteric polymers and clay, greatly contributed to the growth of the particle size before treatment.

Second, hot rolling under 200°C for 16 h might have led to the desorption of cationic groups from bentonite; this could have broken the bridges among the plates and caused a considerable degradation of anionic groups. As a result, $d(0.1)$, $d(0.5)$, and $d(0.9)$ became smaller after thermal aging at 200°C for 16 h. Although amide groups of the AM units might have hydrolyzed

Table VII. Influence of the HPAD-2's Percentage on the Particle Size

HPAD-2 (wt %)	Condition	$d(0.1)$ (μm)	$d(0.5)$ (μm)	$d(0.9)$ (μm)	Dispersity
0	◇	0.445	6.622	86.757	2.90
0	△	0.788	12.626	55.236	1.37
0	▽	1.602	7.402	26.361	1.04
0.5	◇	40.763	137.279	320.234	0.62
0.5	△	17.904	33.108	67.356	0.62
0.5	▽	11.946	28.473	141.822	1.56
1.0	◇	24.002	108.4	243.240	0.61
1.0	△	13.300	31.826	67.382	0.55
1.0	▽	10.975	27.046	275.218	2.22
2.0	◇	21.653	96.758	220.080	0.62
2.0	△	8.188	26.556	100.022	1.53
2.0	▽	9.757	26.776	158.147	1.93
3.5	◇	2.732	40.805	142.823	1.06
3.5	△	2.276	15.672	70.369	1.23
3.5	▽	1.774	11.665	26.398	0.74
4.0	◇	0.886	11.451	87.224	2.47
4.0	△	0.484	6.074	46.386	2.51
4.0	▽	0.910	6.398	19.714	1.06
5.0	◇	0.854	7.695	63.516	2.58
5.0	△	0.316	6.162	22.508	1.27
5.0	▽	0.291	4.343	17.057	1.09

◇, measurements were taken before aging; △, measurements were taken after aging at 200°C for 16 h; ▽, measurements were taken after aging at 60°C for 16 h.

Table VIII. ζ Potential Values of the Clay Suspensions

		ζ potential (mV)	
Suspension	HPAD-2 (wt %)	◇	▽
Freshwater mud	0	−35.78	−26.87
Saltwater mud	0	−37.91	−46.01
Saltwater mud	0.5	−40.74	−40.29
Saltwater mud	1.0	−41.09	−39.99
Saltwater mud	2.0	−41.50	−39.19
Saltwater mud	3.5	−42.62	−37.01
Saltwater mud	4.0	−42.85	−39.07
Saltwater mud	5.0	−42.92	−37.88

◇, measurements were taken before aging; ▽, measurements were taken after aging at 60°C for 16 h.

under a high temperature to replenish the loss of carboxyl groups, the former reaction rate could not compete with the later reaction rate.

Third, the damage by high-speed shearing at 10,000 rpm to the temporarily aggregated clay plates and redispersion at a lower temperature of 60°C caused the clay particles to redistribute. That is why both the particle sizes in Table VII and the rheological properties in Table VI became smaller in the samples after aging under 60°C compared to those before this treatment.

Fourth, the more HPAD-2 was added to mud, the greater the amount of groups with like charges in the drilling fluids was. Anionic groups, in particular, occupied less space in the solution because of their growing repulsion between each other. In balance, repulsive forces prevailed among the polymers, and each polymer chain had less opportunity to link to the particles. That is why the distribution of mud with a higher content of HPAD-2 was narrower than that of the mud with a concentration of additive.

Lastly, a shift in the particle distribution toward a smaller value improved the clay suspension's ability to bridge across the pores and form an effective filter cake. The average pore size of the filter paper simulating formation in the HTHP experiment was less than 20 μm in accordance with SY/T 5677-1993, one of China's industrial standards. The percentage of particles with a size equal to or slighter greater than 6.67 μm (one-third of the pore size) increased when the content of the additive in mud was greater than or equal to 3.5 wt %. An obvious reduction in the filtrate volume was observed when HPAD-2's content exceeded 2.0 wt %; this was in good agreement with the bridging materials selecting rule discussed in a previous work.[28,29]

ζ Potential Test Results

The ζ potentials of mud under different conditions are shown in Table VIII. That ζ potential of freshwater mud enhancement after aging was due to the harm of the high-temperature treatment to the card-house structure of the clay suspension. Clay flakes, therefore, became more dispersed, and the absolute negative charge decreased. The addition of excessive salt enhanced bentonite's aggregation in mud and lowered the ζ potential. This was explained by the simultaneous occurrence of the face-to-face association as a result of the electrolyte's compression of the diffuse double layers of the charged groups at high salinity. The degree of the clay plates' aggregation, therefore, increased and led to a pronounced shift in the ζ potential toward more negative.

The ζ potential of bentonite decreased as the content of HPAD-2 increased before the aging treatment. The greater the amount of additive added to clay suspension was, the smaller the ζ potential became. The explanation was that HPAD-2 bridged across the bentonite plates via the adsorption of positively charged groups onto the faces of particles.[33] The whole charge of HPAD-2, however, was negative because of the greater amount of hydrolyzed AM units compared to that of DMDAAC units in the polymer chain. With increasing additive concentration, the absolute value of the ζ potential increased because more polyampholyte was attached to each clay particle and more negative charge was introduced to the flakes.

The relationship of bentonite's ζ potential with HPAD-2's concentration after the aging treatment, however, was completely the opposite of that before heating. Bentonite's ζ potential moved toward a less negative value as the additive's percentage rose when the thermal treatment was finished. This phenomenon could be explained as follows: the cationic groups were more stable than the anionic groups under high temperatures in accordance with the IR spectra of Table IV and V. The decomposition of the hydrolyzed AM units during hot rolling resulted in a decrement of net negative charge carried by the HPAD-2 polymer chains adsorbed on the clay plates and the degradation of polymers chains, as supported by the intrinsic viscosity data in Table III.

The ζ potential of the salt mud with HPAD-2 that experienced heat treatment was still higher in absolute value than those of the freshwater mud before aging; this indicated that the HPAD-2 polymers protected the clay flakes from aggregation under

Table IX. Properties of the Mud with HPAD-2 and Other Additives

Additive	Heat treatment	Clay (wt %)	Polymer (wt %)	NaCl (wt %)	η_a (mPa s)	η_p (mPa s)	τ_0 (Pa)	API loss (mL)	HTHP loss (mL)
Forpolymer[19]	220°C for 16 h	8.0	1.0	Saturated	13.5	13.0	0.50	37.0	—[a]
HPAD-2	220°C for 16 h	8.0	1.0	Saturated	22.5	18.0	4.60	28.6	—[a]
Forpolymer[19]	200°C for 16 h	8.0	1.0	Saturated	39.0	27.0	11.0	14.0	—[a]
HPAD-2	200°C for 16 h	8.0	1.0	Saturated	26.0	20.0	6.13	20.4	—[a]

[a] The em dash shows that the HTHP experiment temperature was not specified in ref. 19.

Table X. Properties of the HPAD and Mud with HPADs with Different Hydrolysis Degrees

	Net negative charge (mol %)	Cationicity (mol %)	Anionicity (mol %)	η_a (mPa s) ▽	η_p (mPa s) ▽	τ_0 (Pa) ▽	API loss (mL) ▽	HTHP loss (mL) ▽
HPAD-1	19.7	10.3	30.0	73.0	55.0	18.40	5.3	26.6
HPAD-2	30.1	10.3	40.4	81.0	59.0	22.48	2.2	17.4
HPAD-3	39.3	10.3	49.6	64.0	50.0	14.31	3.6	36.5
HPAD-4	41.5	10.3	51.8	67.0	52.0	15.33	3.9	31.8

high temperature. This was in good agreement with the particle size data in Table VII.

Comparison of the Filtration Reduction Abilities between HPAD-2 and Other Additives

Table IX shows the data of the rheological properties and the filtration of saltwater mud with HPAD-2 and the forpolymer of AM, AMPS, NVP, and organosilicon monomer under test conditions from a previous article.[19] With 8.0 wt % bentonite in mud, HPAD-2 performed better than the reported forplymer after aging under 220°C for 16 h but worse when the treatment temperature dropped to 200°C.

HPAD-2, as one type of polyampholyte, owned the ability to control the filtration of the polyelectrolyte with only anionic groups.

Effects of HPAD's Hydrolysis Degree on the Properties of the Mud

The rheological properties and filtration of the mud with HPAD with different hydrolysis degrees, along with the structural information of the polymers, are listed in Table X.

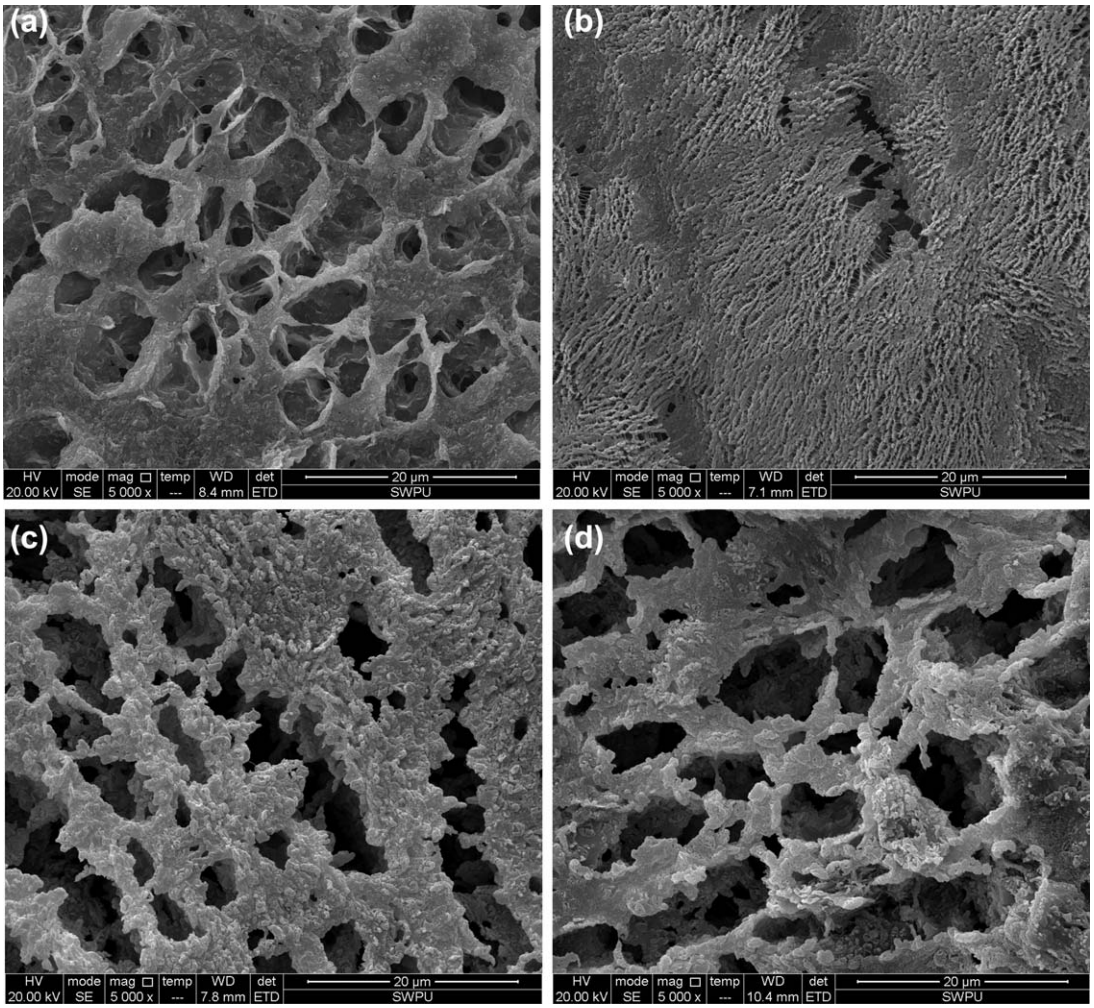

Figure 6. Microstructures of the HTHP filter cakes with HPAD: (a) HPAD-1, (b) HPAD-2, (c) HPAD-3, and (d) HPAD-4.

The performance of the saltwater mud with HPADs with various anionicities, including the viscosity and filtrate volume, improved at first when COO^-'s content increased, but it dropped later as the anionicity grew bigger. HPAD-2, with an anionicity of 40.4 mol %, a net negative charge of 30.1 mol % in other words, did the best in controlling the water loss of the mud with a high salinity.

Scanning Electron Microscopy Microstructure Observation

Figure 6 displays the microstructure of the HTHP filter cakes. The cracks were the place occupied by H_2O molecules before sample preparation. The polymers existed as bridges connecting adjacent clay particles on the surface of the cake.

HPAD's polymer chains could be found in the surface of the four HTHP filtrate cakes, except that the polymer distribution density was relatively lower in the case of HPAD-3 and HPAD-4 than in HPAD-1 and HPAD-2. Second, the average size of cavities in the HTHP filtrate cakes of HPAD-3 and HPAD-4 was considerably larger than those of HPAD-1 and HPAD-2. Third, the HPAD-2 polymers distributed the most uniformity in the surface of the clay particles among all four polyampholytes; this not only helped narrow the cracks between adjoined clay flakes but also increased the retention time of the water molecules through the filter cake. We reached the conclusion that when more bridges were formed by polymers across bentonite and the cavities were smaller, the drilling fluid performed better in the HTHP filtration experiment. This result was in agreement with the fact that the saltwater drilling fluid with HPAD-2 had the lowest API and HTHP filtration as per Table X.

CONCLUSIONS

An amphoteric filter loss reducer for saltwater-based drilling fluids, named HPAD, was synthesized by solution polymerization and characterized by IR and NMR methods. The IR spectroscopy confirmed the presence of DMDAAC segments in HPAD with the peak at 1460 cm^{-1} and the successfully hydration of $-CONH_2$ with the peak at 1560 cm^{-1}. The NMR results provided another piece of evidence that the structure of HPAD consisted of DMDAAC, AM, and hydrolyzed AM segments. The TGA curves revealed that the HPAD's resistance to heat under the N_2 condition was better than that with both N_2 and O_2. The instability of HPAD with O_2's presence required the addition of Na_2SO_3 to the clay suspensions; this was demonstrated by the intrinsic viscosity experiments of the HPAD aqueous solution with and without Na_2SO_3 after aging treatment.

A high salinity, namely, 30 wt % NaCl, significantly impaired the rheological properties and enhanced the filtration of the mud. The addition of HPAD increased the viscosity of mud and reduced the API and HTHP filter volume after the aging test. These indices became better as HPAD-2's content increased. The API and HTHP filtrations dropped to 2.2 and 17.4 mL, respectively, when HPAD-2's percentage reached 3.5 wt %.

The particle size tests of mud after aging showed that the increase in this additive's concentration made the medium size shift toward a smaller value, bentonite's bridging ability across the pores improved, and the mud's filtration decreased. This amphoteric polymer's interaction with clay particles was further investigated by ζ potential tests, in which HPAD's addition lowered the particles' ζ potential, and helped to stabilize the clay suspension.

The hydrolysis degree of HPAD had to be controlled in a proper range, 30.1 mol % of net negative charge, to optimize its ability to control water loss. Scanning electron microscopy photos of the microstructure of the HTHP filter cakes showed that the HPAD-2 with a net negative charge of 30.1 mol % had the best performance in the control of saltwater mud's filtration.

The influence of the HPAD structural parameters, including the cationicity, anionicity, and polymer weight, on the mud's rheological properties and filtration, along with the mechanism of HPAD's adsorption to the clay particles, will be studied in our future research work.

REFERENCES

1. Zhuang, Y.; Zhu, Z.; Chao, H.; Yang, B. *J. Appl. Polym. Sci.* **1995**, *55*, 1063.
2. Collette, C.; Lafuma, F.; Audebert, R.; Brouard, R. *J. Appl. Polym. Sci.* **1994**, *53*, 755.
3. Fordham, E. J.; Ladva, H. K. J. *J. Colloid Interface Sci.* **1992**, *148*, 29.
4. Jiao, D.; Sharma, M. M. *J. Colloid Interface Sci.* **1994**, *162*, 454.
5. Wu, Y. F.; Mahmoudkhani, A.; Watson, P.; Fenderson, T. R.; Nair, M. Presented at SPE EOR Conference at Oil and Gas West Asia, Muscat, Oman, April **2012**; Paper SPE 155653.
6. Dai, C.; You, Q.; He, L.; Zhao, F. *Energy Source Part A* **2011**, *34*, 53.
7. Zhang, L. M.; Tan, Y. B.; Li, Z. *Colloid Polym. Sci.* **1999**, *277*, 1001.
8. Iscan, A. G.; Kok, M. V. *Energy Source Part A* **2007**, *29*, 939.
9. Zhang, L. M. *Starch* **2001**, *53*, 401.
10. Eutamene, M.; Benbakhti, A.; Khodja, M.; Jada, A. *Starch* **2009**, *61*, 81.
11. Salami, O. T.; Plank, J. *J. Appl. Polym. Sci.* **2013**, *129*, 2544.
12. Kelessidis, V. C.; Papanicolaou, C.; Foscolos, A. *Int. J. Coal Geol.* **2009**, *77*, 394.
13. Kelessidis, V. C.; Tsamantaki, C.; Michalakis, A.; Christidis, G. E.; Makri, P.; Papanicolaou, K.; Foscolos, A. *Fuel* **2007**, *86*, 1112.
14. Mortimer, D. A. *Polym. Int.* **1991**, *25*, 29.
15. Wu, Y. M.; Sun, D. J.; Zhang, B. Q.; Zhang, C. G. *J. Appl. Polym. Sci.* **2002**, *83*, 3068.
16. Wu, Y. M.; Zhang, B. Q.; Wu, T.; Zhang, C. G. *Colloid Polym. Sci.* **2001**, *279*, 836.
17. Peng, B.; Peng, S. P.; Long, B.; Miao, Y. J.; Guo, W. Y. *J. Vinyl Addit. Technol.* **2010**, *16*, 84.
18. Guo, W. Y.; Peng, B. *J. Vinyl Addit. Technol.* **2012**, *18*, 261.
19. Chu, Q.; Luo, P. Y.; Zhao, Q. F.; Feng, J. X.; Kuang, X. B.; Wang, D. L. *J. Appl. Polym. Sci.* **2013**, *128*, 28.

20. Nunes, R. D. C. P.; Pires, R. V.; Lucas, E. F.; Vianna, A.; Lomba, R. *J. Appl. Polym. Sci.* **2014**, *131*, 40646.
21. Han, H. F.; Zhang, J. H. *J. Appl. Polym. Sci.* **2013**, *130*, 4608.
22. Kudaibergenov, S. E. *Adv. Polym. Sci.* **1999**, *144*, 115.
23. Ma, Z.; Li, Q.; Yue, Q.; Gao, B.; Xu, X.; Zhong, Q. *Bioresour. Technol.* **2011**, *102*, 2853.
24. Chen, S. T.; Vaughan, C. W. U.S. Pat. 5,609,862 **1997**.
25. Lu, S.; Liu, R.; Sun, X. *J. Appl. Polym. Sci.* **2002**, *84*, 343.
26. Anderson, R. L.; Ratcliffe, I.; Greenwell, H. C.; Williams, P. A.; Cliffe, S.; Coveney, P. V. *Earth-Sci. Rev.* **2010**, *98*, 201.
27. Wang, Q.; Dan, Y.; Wang, X. G. *Pure Appl. Chem.* **1997**, *34*, 1155.
28. Abrams, A. *J. Petrol. Technol.* **1977**, *29*, 586.
29. Smith, P. S.; Browne, S. V.; Heinz, T. J.; Wise, W. V. Presented at SPE Annual Technical Conference, Denver, Colorado, **1996**; Paper SPE 36430.
30. Abdollahi, M.; Ziaee, F.; Alamdari, P.; Koolivand, H. *J. Polym. Res.* **2013**, *20*, 239.
31. Wang, X.; Yue, Q.; Gao, B.; Si, X.; Sun, X.; Zhang, S. *J. Appl. Polym. Sci.* **2011**, *120*, 1496.
32. Shi, Y.; Zhan, X. C.; Lv, T. P.; Li, L.; Cao, C. Y.; Shu, X. M.; Li, C. R.; Li, L. L. *Acta Chim. Sinica* **2006**, *64*, 496.
33. Zhang, L. M.; Yin, D. Y. *J. Appl. Polym. Sci.* **1999**, *74*, 1662.